

CALIFORNIA POLYTECHNIC STATE UNIVERSITY, SAN LUIS OBISPO

Mechanical Engineering Department

Heat Transfer Lab, ME 343-07

TO: Mr. Hontz

FROM: Team 3

SUBJECT: Air-to-Air Heat Exchanger

Description: This experiment introduces the basic operation of the air-to-air heat exchanger shown in for both parallel flow and counter flow conditions and compares experimental and modeled performance characteristics.

DATE OF EXPERIMENT: March 7, 2023

DATE SUBMITTED: March 21, 2023

TEAM MEMBERS AND THEIR DUTIES:

Harrison Pomerantz Assistant

Anthony Mendoza Assistant

Joseph Penrose Assistant

Christopher Ng Assistant

Table of Contents

1.	Summary/Objective	Page 3
2.	Equipment and Methods	Page 4-6
3.	Data and Result/Discussion	Page 6-20
4.	Conclusions	Page 19
5.	Bibliography	Page 20
6.	Appendix A	Page 21
7.	Appendix B	Page 22
8.	Appendix C	Page 23
9.	Appendix D	Page 24

SUMMARY AND OBJECTIVE

Heat exchangers are used to move thermal energy from one fluid to another, many times for the purposes of cooling. Such examples include radiators in cars for engine cooling and air conditioners. The objectives of this experiment were to introduce the basic operation of an air-to-air heat exchanger for both parallel flow and counter flow conditions and compare experimental and modeled performance characteristics. We used fluid and wall temperature measurements to calculate the actual performance parameters such effectiveness, ϵ , and NTU, number of transfer units, and then compared these values to those predicted using modeling and previously developed correlations. We modeled the heat exchanger using the log mean temperature difference method, which can be used to predict the heat transfer between the inner and outer streams, the outlet temperatures, and the heat exchanger effectiveness given the size and inlet conditions. For this model to be applicable, the following assumptions needed to be made: uniform cross-sectional properties, perfectly insulated exterior, negligible axial conduction in each fluid and changes in potential and kinetic energy, and constant specific heats and convection coefficients. As stated before, two different flow configurations were considered: parallel flow and counter flow. As for the experiment itself, the counterflow configuration performed better than the parallel configuration. This was seen in the results as a higher change in temperature in the cold air annulus with counterflow, as well as the values of heat transfer out of the hot air and the heat transfer into the cold air being closer together. The differences in the experimental heat transfer values from the two sides of the heat exchanger were the result of losses, including heat transfer from the cold air to the ambient air. Overall, there was good agreement between the model and our experiment.

EQUIPMENT

The following list of equipment was used in the experiment

- Heat exchanger apparatus, shown in Figure 1. below
- Stainless steel tubing (3/8 in OD, 0.319 in ID, 6 ft length)
- PVC clear pipe (1 in-SCH 40, approximate 1 ft length sections)
- 2 Flowmeters
- Air process heater
- Digital controller
- 8 Type-T Thermocouples
- DAQ module

This test was carried out with this equipment in the test-rig depicted below:

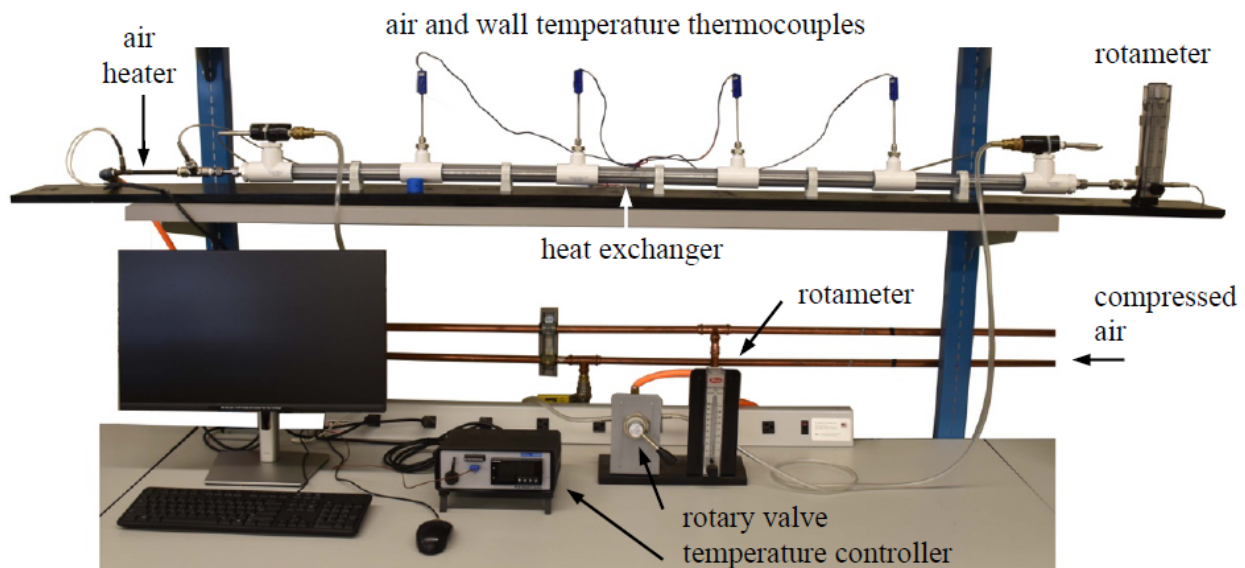


Figure 1 - Labeled Diagram of the Air-to-Air Heat Exchanger, taken from ME 343 Heat Transfer Laboratory Manual

METHODS

The schematic with the control volume and relevant measured quantities is provided in Figure 2.

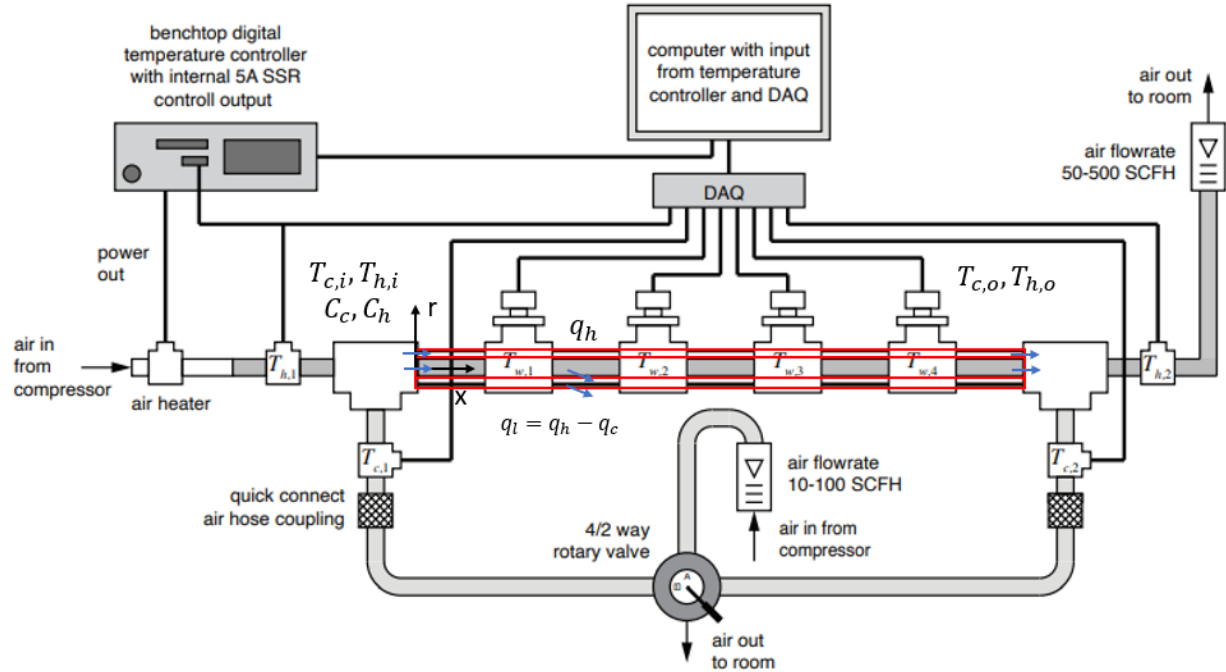


Figure 2 - Annotated Schematic Diagram of the Air-to-Air Heat Exchanger

In this experiment, the goal is to use temperature and mass flow rate data to calculate heat transfer out of the air inside the pipe. As such, both temperature and flow rate were measured throughout the experiment for both parallel and counterflow configurations. For both the hot and cold airflows, the volumetric flowrate was measured and controlled using an in-line rotameter with a built-in control valve. Flowrate through the cold air annulus was held at a nominal value of 100 scfh, or standard cubic feet per hour. The flow rate of the hot air was varied between the nominal values of 100 and 400 scfh at 100 scfh intervals. For temperature data, inlet (1) and outlet (2) temperatures were recorded for the hot and cold flows. In addition, the temperature of the walls of the internal hot air tube were recorded. All flow rate and temperature measurements were recorded with the provided DAQ (data acquisition system). The data was then transferred to the team's personal systems for processing and analysis.

DATA AND RESULTS AND DISCUSSION

Due to a malfunction in the STE, legacy data was provided by Mr. Hontz. Initial data processing in Excel was required to convert all temperatures and pressures to absolute. We can then use the mean temperature difference between the entrance and exit of the CVs for the hot and cold air, as seen in Figure 2, to obtain the properties of the air at each flow rate using EES's property tables.

First Law of Thermodynamics Method

Using the data in Appendix A, we must first correct the volumetric flowrates of the hot and cold air using the rotameters' air properties and Equation 1, then Equation 2 for the corrected mass flowrates going through the rotameters.

$$Q_{rot} = \frac{Q_{cal}}{\sqrt{\left(\frac{P_{rot}}{P_{cal}}\right)\left(\frac{T_{cal}}{T_{rot}}\right)}} \quad (1)$$

$$m_{dot} = \rho_{rot} * Q_{rot} \quad (2)$$

- Q - Volumetric Flowrate (scfh)
- m_{dot} - Calibration to Rotameter Temperature (kg/s)
- $\frac{P_{rot}}{P_{cal}}$ - Rotameter to Calibration Pressures ~1
- $\frac{T_{cal}}{T_{rot}}$ - Calibration to Rotameter Temperature
- ρ_{rot} - Rotameter Air Density (kg/m³)

By analyzing our two control volumes of hot air and cold air, we can apply conservation of energy to produce Equations 3 and 4 which can be used to calculate the experimental overall heat transfer between and out of the two control volumes.

$$q_h = \dot{m}_h c_{p,h} (T_{h,i} - T_{h,o}) = C_h \Delta T_h \quad (3)$$

$$q_c = \dot{m}_c c_{p,c} (T_{c,o} - T_{c,i}) = C_c \Delta T_c \quad (4)$$

- q - Heat Transfer Rate (Watts)
- C - Fluid Heat Capacity $\dot{m}_{dot} * c_p$ (J/s²K)

To justify further analysis, we need to determine the Nusselt and Reynold's numbers for this system. For the hot air's internal pipe flow, since the Nusselt Number definition changes if the flow is turbulent or laminar, we first need to check if the Reynolds Number, using Equation 5, is greater than 2300 for laminar flow to use the modified Dittus Boetler correlation in Equation 6. Equation 6 also gives us h once the Nusselt number is calculated. We also need to evaluate the cold air's internal annular flow. Note that the Reynold's number was calculated with air properties evaluated at the Air's Bulk Temperature. Additionally, when finding the Nusselt number using the Dittus Boetler equation, the Prandtl Number was evaluated at the film temperature.

$$Re_{D_h} = \frac{\rho \bar{V} D_h}{\mu} \quad \text{where} \quad D_h = 4 A_c/P \quad (5)$$

$$Nu_D = 0.023 Re_D^{4/5} Pr^n = \frac{h D_h}{k_f} \quad (6)$$

- Re_D - Reynolds Number with Air Properties Evaluated at the Air's Bulk Temperature
- \bar{V} - Average Velocity (m/s)
- D_h - Hydraulic Diameter (m)
- Nu_{D_h} - Nusselt Number with Air Properties Evaluated at the Air's Film Temperature. For Cold Air, either ~ 6.67 for Constant Surface Temperature and Laminar Flow or ~ 7.25 for Constant Heat Flux and Laminar Flow
- Pr - Prandtl Number (evaluated at film temperature)
- $n = 0.3$ for Cooling
- h = Convection Coefficient of Air, $W/(m^2 * K)$
- K_f = Thermal Conductivity of Air, $W/(m * K)$

In Appendix D's example calculation, we find the Reynolds Number to be 1748 which allows us to use values for annulus flow which is 6.67 for constant surface temperature and laminar flow with an inner diameter to outer diameter ratio of 0.357. Note that for the Parallel Flow Laminar case, the constant wall temperature value was used for Nusselt number. For the Counter Flow case, the constant surface heat flux value was used for the Nusselt number. The assumptions of constant surface heat flux or constant wall temperature is discussed more, and visualized in Figure 3. The results of Equations 1-6 are provided in Table 1.

Table 1 - Experimental Results of Mass and Heat Flow Rates

PARALLEL FLOW											
Measured Volumetric Flow Rate, Q (scfh)		Actual Volumetric Flow Rate, Q (scfh)		Actual Mass Flow Rate, m_{dot} (kg/s)		Reynold's Number, Re		Nusselt Number, Nu		Convection Coefficient, h (W/m ² *K)	
Cold	Hot	Cold	Hot	Cold	Hot	Cold	Hot	Cold	Hot	Cold	Hot
100	100	100.9	102.7	0.000917	0.000902	1748	7137	6.67	24.98	10.11	85.33
100	200	101.3	207.3	0.000914	0.001786	1742	14138	6.67	43.17	10.11	147.43
100	300	101.5	312.5	0.000912	0.002666	1739	21106	6.67	59.48	10.11	203.14
100	400	101.5	417.7	0.000912	0.003546	1738	28068	6.67	74.71	10.11	255.18

COUNTER FLOW											
Measured Volumetric Flow Rate, Q (scfh)		Actual Volumetric Flow Rate, Q (scfh)		Actual Mass Flow Rate, m_{dot} (kg/s)		Reynold's Number, Re		Nusselt Number, Nu		Convection Coefficient, h (W/m ² *K)	
Cold	Hot	Cold	Hot	Cold	Hot	Cold	Hot	Cold	Hot	Cold	Hot
100	100	99.9	102.8	0.000917	0.000902	1706	7043	7.25	24.97	11.07	85.33
100	200	99.9	207.5	0.000914	0.001786	1706	13949	7.25	43.13	11.07	147.40
100	300	99.9	312.6	0.000912	0.002666	1707	20840	7.25	59.46	11.07	203.23
100	400	99.8	417.9	0.000912	0.003546	1707	27710	7.25	74.68	11.07	255.26

To visualize the heat transfer occurring in the STE, air and wall temperatures were plotted against axial location for the lowest flow rate in both directions. This plot is provided in Figure 3.

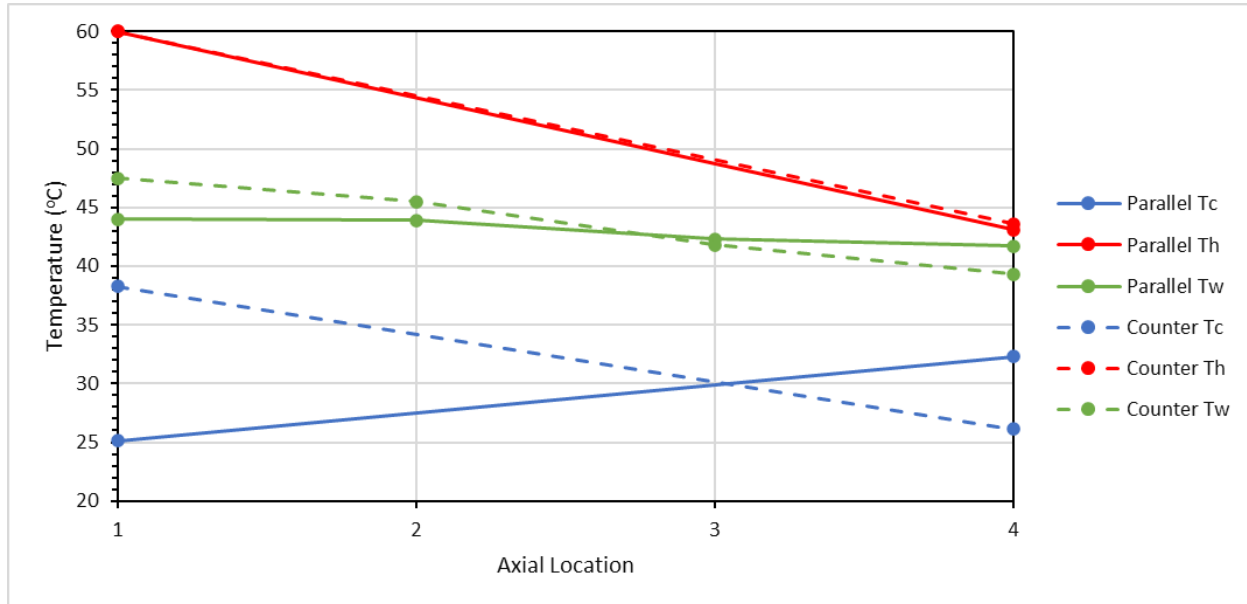


Figure 3 - Experimental Temperatures vs Axial Location at Lowest Hot Air Flow Rate

The trends shown in the plot are what we expected. For parallel flow, the trend is very intuitive – the delta is wide at the entrances, and the temperatures tend to converge as they pass heat to each other. Additionally, note that the T_w is constant, which is why we used the constant surface temperature condition for determining the Nusselt number for the laminar flow, parallel flow case. For counter flow, the cold air is going from 4 to 1, so its temperature increases towards 1. Note that the ΔT across the hot and cold flows for the counter flow is about constant. This constant ΔT also suggests a constant surface heat flux, which is why we used the constant surface heat flux condition when determining the Nusselt number for the laminar flow, counter flow case. The wall follows a similar trend for both flows, which is expected because the hot air always goes one way and drives the wall temperature in that direction. The fact that the slope of the wall temperature is different suggests that the heat transfer is different, which we also saw. To get a better look at the flow rate dependence and temperature change, the temperature deltas from end-to-end for both air flows in both directions were plotted against volumetric flow rate in Figure 4.

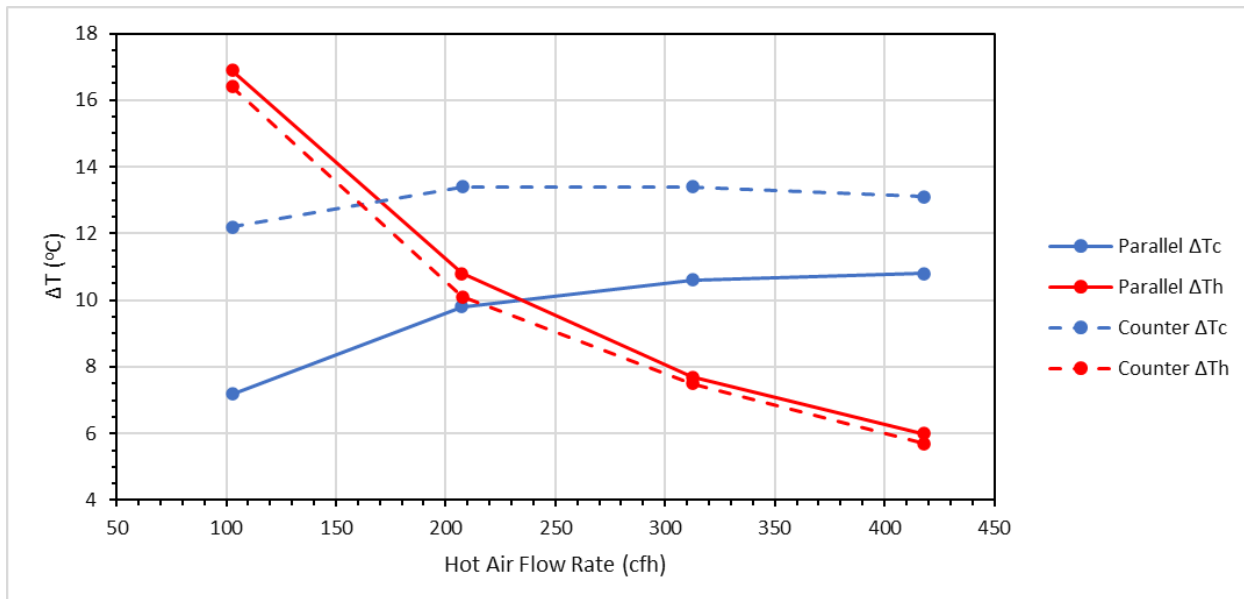


Figure 4 - Experimental Temperature Deltas vs Volumetric Flow Rate

The trends in the plot show that the counter flow setup causes a stronger change in the cold air temperature. This suggests that the cold air receives greater heat transfer in counter flow. For all curves, there appears to be an asymptotic limit to the heat transfer, suggesting that there is an upper limit to effectiveness in terms of increasing flow rate. To really lock down these trends, the heat transfer rates from end-to-end for both air flows in both directions were plotted against volumetric flow rate in Figure 5

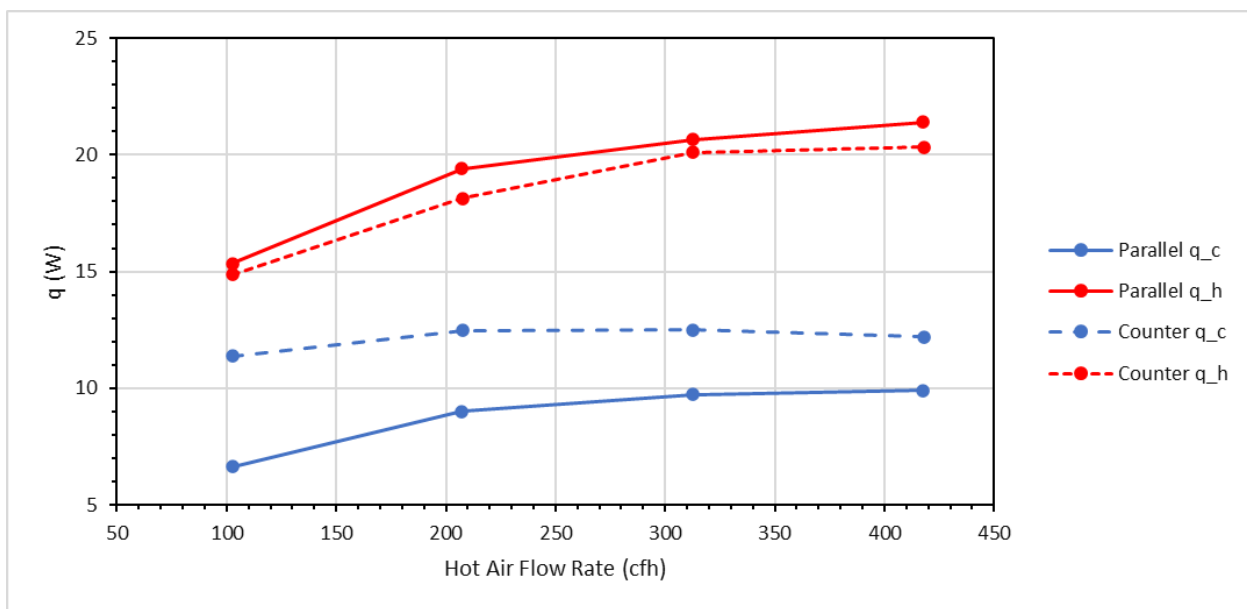


Figure 5 - Experimental Heat Transfer Rates vs Volumetric Flow Rate

The trends in this plot appear to confirm what was expected previously. There may be an upper limit to the heat transfer rate in terms of increasing flow rate. We also see a large change in cold air heat transfer in counter flow, which suggests it's a more effective configuration. However, the hot air has the opposite result. There is an issue that is very obvious on this plot specifically – for a perfectly insulated system, the heat transfer rates should be the same. We do not observe this. It must be, then, that the cold air is losing a great deal of heat somewhere other than the hot air stream. We suspect that another convection - conduction - convection series of thermal

resistances occur at the PVC interface with lab air, causing a significant amount of heat to be lost out of the STE. This may be corroborated by measuring the temperature of the outer PVC pipe and confirming whether or not it is hot enough for buoyancy-driven convection to be occurring to such an extent that it would explain the discrepancy shown here.

Determining the Overall Convection Coefficients

These heat transfer values will later be used with Newton's Law of Cooling to solve for an overall convection coefficient, U , as well as the dimensionless effectiveness parameters in Equation 7.

$$\varepsilon_h = \frac{q_h}{q_{max}}, \quad \varepsilon_c = \frac{q_c}{q_{max}}, \quad q_{max} = C_{min}(T_{h,i} - T_{c,i}) \quad (7)$$

- ε - Heat Exchanger Effectiveness

Knowing our experimental heat transfer rates, we can now calculate the convection coefficients for both parallel and counter flow. Through differential analysis of the fluid, we find Equation 8 for both flow cases, where due to a changing mean temperature to wall temperature difference, we must instead use the log-mean temperature difference, ΔT_{lm} . The definitions for ΔT_1 and ΔT_2 , do however change from $\Delta T_1 = T_{h,i} - T_{c,i}$ and $\Delta T_2 = T_{h,o} - T_{c,o}$ to $\Delta T_1 = T_{h,i} - T_{c,o}$ and $\Delta T_2 = T_{h,o} - T_{c,i}$ for counter flow.

$$q = U A \Delta T_{lm} \quad (8)$$

$$\Delta T_{lm} = \frac{(\Delta T_2 - \Delta T_1)}{\ln(\Delta T_2 / \Delta T_1)}$$

- U - Overall Coefficient of Convection (W/m^2K)
- A - Surface Area of Convection Between the Two Fluids (m^2)
- ΔT_{lm} - Log-Mean Temperature Difference (K)

This overall coefficient can then be used to calculate the NTU which will be compared to later

$$NTU = \frac{UA}{C_{min}} \quad (9)$$

- C_{min} - Minimum Heat Capacity
- A - Surface Area Experiencing Convection

ε -NTU Method

The second model that we can compare the heat exchanger effectiveness to is the ε -Number of Transfer Units Method. To use this method, we need to determine the local convection coefficients for the hot air and cold air through the use of the unitless Nusselt Number. We confirmed these numbers to be valid previously in Table 1. The local convection coefficients can be calculated, and from Newton's Law of Cooling, we can use the convection coefficients and can assume the stainless-steel has negligible thermal resistance, R_w .

$$\frac{1}{UA} = \frac{1}{(hA)_h} + R_w + \frac{1}{(hA)_c} \quad (10)$$

From here, we can use Equations 9 and 11 to calculate the NTU , C_r , and ε to compare ε -NTU model to our experimental conservation of energy calculation.

$$\varepsilon = \begin{cases} \frac{1 - \exp[-\text{NTU} (1 - C_r)]}{1 - C_r \exp[-\text{NTU} (1 - C_r)]} \\ \frac{\text{NTU}}{(1 + \text{NTU})} \text{ for } C_r = 1 \end{cases} \quad (11)$$

where

$$C_r = C_{min}/C_{max} \leq 1$$

- C_r - Heat Capacity Ratio for Multi Stream Heat Exchangers

The results of Equations 7-11 are provided in Table 2.

Table 2 - Experimental Overall Performance Coefficients for the Hot and Cold Air in (a) Parallel and (b) Counter Flow

PARALLEL FLOW											
Actual Volumetric Flow Rate, Q (scfh)		Overall heat transfer coefficient, U (W/m ² -K)			Number of Transfer Units, NTU			Heat Exchanger Effectiveness, ε			
Cold	Hot	Cold	Hot	Total	Cold	Hot	Total	Cold	Hot	Total	
100.9	102.7	7.19	16.61	9.59	0.3558	0.8227	0.4394	0.2095	0.4844	0.2932	
101.3	207.3	8.60	18.54	10.11	0.4206	0.9068	0.4575	0.2792	0.6020	0.3303	
101.5	312.5	8.79	18.67	10.32	0.4304	0.9147	0.4678	0.3037	0.6454	0.3474	
101.5	417.7	8.68	18.78	10.44	0.4255	0.9203	0.4734	0.3112	0.6731	0.3568	

COUNTER FLOW											
Actual Volumetric Flow Rate, Q (scfh)		Overall heat transfer coefficient, U (W/m ² -K)			Number of Transfer Units, NTU			Heat Exchanger Effectiveness, ε			
Cold	Hot	Cold	Hot	Total	Cold	Hot	Total	Cold	Hot	Total	
99.9	102.8	12.96	16.95	6.92	0.6422	0.8400	0.3174	0.3699	0.4838	0.2417	
99.9	207.5	12.57	18.26	7.33	0.6061	0.8802	0.3270	0.3953	0.5741	0.2615	
99.9	312.6	11.87	19.12	7.50	0.5720	0.9215	0.3344	0.3941	0.6349	0.2721	
99.8	417.9	11.09	18.46	7.59	0.5344	0.8897	0.3385	0.3842	0.6396	0.2778	

What we observe from these results is that we have two experimental values for everything using the First Law of Thermodynamics method due heat losses in the experiment compared to the ε -NTU Method which assumes the system is insulated to its surroundings.

For all three major parameters of interest, the overall heat transfer coefficient (U), the Number of Heat Transfer Units (NTU) and the Heat Exchanger Effectiveness (ε), we notice that the magnitude of the hot parameters (U_h , NTU_h , and ε_h), are all greater than the respective magnitudes of the cold side parameters (U_c , NTU_c , and ε_c) for all volumetric flow rates and flow directions. This matches our expectations since we know that the hot air side heat transfer value is greater than the cold-air side, because the cold-air side experiences losses (previously discussed). Because of this, it is very clear that the hot-air side effectiveness (ε_h) will be greater than the cold side effectiveness (ε_c) (direct proportionality shown by Equation 7). Additionally, because both the cold- and hot- air sides have similar changes in temperature, we know through Equation 8, that U_h must also be larger than U_c . As a results, because NTU is calculated based on U_h and U_c , and we expect U_h to be greater than U_c , this confirms our data that the NTU_h is greater than NTU_c . This matches our expectation since NTU is a ratio of the ability to transfer heat to the ability to absorb it. Because we observe a higher heat transfer and temperature for the hot air, it makes sense that its NTU value will be greater than the cold-air side NTU value.

Additionally, we see a trend that shows U_h and ε_h increase with Flowrate. This makes sense since since U is a function of Reynold's number, and Reynold's number increases with flowrate. Similarly, ε_h is a function of m_dot . As flow rate increases, m_dot also increases, which explains why ε_h increases with flowrate. NTU is not as straightforward, since it is a function of both U , which increases with flowrate, and m_dot , which also increases with flowrate. That would explain why the trend is not as clear for that data.

Comparing the overall heart transfer coefficient (U), the overall Number of Heat Transfer Units (NTU), and the Heat Exchanger Effectiveness (ε) to the respective hot-air side components of

these parameters, we notice that the magnitude of the hot parameters (U_h , NTU_h , and ε_h), are all greater than the respective magnitudes of the overall parameters (U , NTU , ε).

Looking at just the overall heat transfer coefficients, this makes sense since when we look at U_h , we are only looking at the convective thermal resistance due to the hot fluid. Comparing this to when we are looking at the overall heat transfer coefficient, we are taking into account the convective thermal resistance of the hot fluid and the convective thermal resistance of the cold fluid (in theory we would also consider the conductive resistance through the steel tube wall however we are assuming this is negligible for this experiment). Another reason for the difference in these values is because we used a mean temperature, mean density, and mean velocity for caluclations to solve for the overall heat transfer coefficient. For the U_h value, it was calculated beased on q_c , which was determined using properties evaluated at the film temperature. While these properties are relatively similar, they are different enough to cause significant differences. One more factor for a difference in values is that our model for U doesn't consider the heat loss to the outside air, while our U_h and U_c do.

This reasoning for why U_h is consistently higher than the overall U extends to the same observation for NTU/NTU_h , and $\varepsilon/\varepsilon_h$. Because the NTU is calculated based on U , it is clear that if U_h is consistently greater than U , than NTU_h will be consistently greater than NTU (shown by directly proportional relationship in Equation 9). By analyzing equation 11, it can be observed that over our range of data values, as NTU increases, the effectiveness increases. Therefore, this explains why ε_h is consistently greater then the overall Effectiveness, ε .

Assumption Justification and Verification

To use the ε -NTU Method, we have to confirm that the flow for the hot and cold air is both hydrodynamically and thermally fully developed for laminar or turbulent flow. This can be done by evaluating the Reynolds Number and then the length to hydraulic diameter ratio, L/D_h , of 160 for the annulus and inner tube. First, we need to organize the geometries involved with the STE. The definitions are shown in Figure 6.

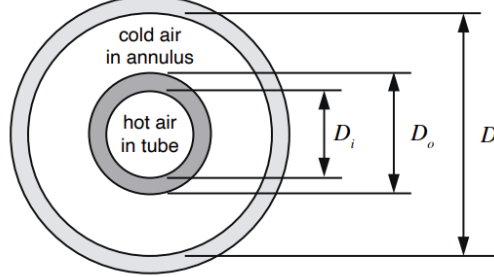


Figure 6 - STE Diameters

The critical geometries are tabulated in Table 3.

Table 3 - Experimental Critical Geometries

Geometry							
D	Di	Do	Dh,c	Dh,h	A,c	A,h	A,s
(m)	m	m	m	m	m ²	m ²	m ²
0.0266	0.00811	0.00953	0.01707	0.00811	4.844E-04	5.166E-05	0.044909

Table 1 shows our calculated Reynolds Numbers for the cold and hot air, and we found the annular cold air flow to be laminar with the hot air flow to be turbulent in both setups. Equations 12 and 13 can be used for the laminar cold air flow and Equations 14 and 15 can be used for the turbulent hot air flow.

$$\left(\frac{L}{D_h}\right)_{hydro} > 0.05Re_{D_h} \quad (12)$$

$$\left(\frac{L}{D_h}\right)_{thermo} > 0.05PrRe_{D_h} \quad (13)$$

$$\left(\frac{L}{D_h}\right)_{hydro} > 1.36Re_{D_h}^{0.25} \quad (14)$$

$$\left(\frac{L}{D_h}\right)_{thermo} > 10 \quad (15)$$

From our experimental Reynolds and Prandtl Numbers, we find the results in Table 4.

Table 4 - Experimental Flow Development Criteria

PARALLEL FLOW			
Laminar Cold Air		Turbulent Hot Air	
0.05Re	0.05PrRe	1.36Re ^{0.25}	
87.4	63.5	12.5	
87.1	63.3	14.8	
86.9	63.2	16.4	
86.9	63.2	17.6	

COUNTER FLOW			
Laminar Cold Air		Turbulent Hot Air	
0.05Re	0.05PrRe	1.36Re ^{0.25}	
85.3	62.0	12.5	
85.3	62.0	14.8	
85.3	62.0	16.4	
85.4	62.0	17.6	

Note that all results are less than 87.9 and 185.0 for the cold and hot length to hydraulic diameter ratios, respectively, verifying that we can use our calculations for the ε -NTU Method.

CONCLUSION

In this experiment, we used fluid and wall temperature measurements to calculate the actual performance parameters of an air-to-air heat exchanger in parallel and counterflow configurations, and then compared these values to those predicted using modeling and previously developed correlations. We modeled the heat exchanger using the log mean temperature difference method, which required certain assumptions. These assumptions were: uniform cross-sectional properties, perfectly insulated exterior, negligible axial conduction in each fluid and changes in potential and kinetic energy, and constant specific heats and convection coefficients. Both temperature flows were also considered to be thermally and hydrodynamically fully developed, an assumption which was shown to be correct between Tables 4 and 5. The cold air flow in the parallel and counterflow configurations was laminar, while the hot air was always turbulent. As for the experiment itself, from Figures 3 and 4, it is clear that the cold air absorbs more heat from the hot air in the counterflow condition compared to the parallel flow configuration. This is seen in the overall change in temperature from between points 1 and 4 in Figure 3, as well as the greater ΔT_c for counterflow in Figure 4. This result is further reinforced in Figure 5, where the values of heat transfer from the hot air to the cold air (q_h) is closer to the values of heat transfer to the cold air from the hot air (q_c) for counterflow compared to parallel flow. That being said, the values between q_c and q_s were not equal, indicating losses in the system. Since the average temperature in the cold air annulus is warmer than the ambient air temperature, there was heat transfer that occurred from the cooling air to the ambient air. This fact is not accounted for in our model, which explains some of the difference seen between q_c and q_h . Overall, there was good agreement between the model and our experiment.

REFERENCES

1. *ME 343 Heat Transfer Laboratory*, 6th Edition, Cal Poly Mechanical Engineering Department, San Luis Obispo, CA, 2022.
2. Moran, M. J, Shapiro, H. N., Boettner, D. D., and Bailey, M. B., *Fundamentals of Engineering Thermodynamics*, 7th Edition, John Wiley & Sons, New York, 2011.
3. Bergman, T. L, Lavine, A. S, *Fundamentals of Heat and Mass Transfer*, 8th Edition, John Wiley & Sons, New York, 2017.
4. *Engineering Equation Solver*, F-Chart Software, 2023.

APPENDIX

APPENDIX A

Tabulated Raw Data

RAW DATA									
PARALLEL FLOW									
Qc (scfh)	Qh (scfh)	Tc,1 (°C)	Tc,2 (°C)	Th,1 (°C)	Th,2 (°C)	Tw,1 (°C)	Tw,2 (°C)	Tw,3 (°C)	Tw,4 (°C)
100	100	25.1	32.3	60.0	43.1	44.0	43.9	42.3	41.7
100	200	24.9	34.7	60.0	49.2	46.4	46.6	45.5	45.4
100	300	25.1	35.7	60.0	52.3	47.5	48.5	47.3	47.5
100	400	25.3	36.1	60.0	54.0	48.8	49.5	48.6	49.0

COUNTER FLOW									
Qc (scfh)	Qh (scfh)	Tc,1 (°C)	Tc,2 (°C)	Th,1 (°C)	Th,2 (°C)	Tw,1 (°C)	Tw,2 (°C)	Tw,3 (°C)	Tw,4 (°C)
100	100	38.3	26.1	60.0	43.6	47.5	45.5	41.8	39.3
100	200	39.5	26.1	60.0	49.9	50.6	49.6	46.2	44.4
100	300	39.4	26.0	60.0	52.5	51.2	50.6	47.7	46.4
100	400	39.0	25.9	60.0	54.3	51.5	51.5	48.7	47.5

Table A.1 - Raw Data Collected

APPENDIX B

Converted Data, Rotameter Correction & Heat Transfer Calculations

CORRECTED DATA											
PARALLEL FLOW											
Qc (act)	rho_c (rot)	mdot_c	C_c	DELTA.Tc	q_c	Qh (act)	rho_h (rot)	mdot_h	C_h	DELTA.Th	q_h
(scfh)	(kg/m3)	(kg/s)	(W/K)	(K)	(W)	(scfh)	(kg/m3)	(kg/s)	(W/K)	(K)	(W)
100.9	1.156	0.0009174	0.922	7.2	6.63	102.7	1.116	0.0009016	0.907	16.9	15.33
101.3	1.147	0.0009138	0.918	9.8	9.00	207.3	1.095	0.001786	1.797	10.8	19.40
101.5	1.143	0.0009123	0.917	10.6	9.72	312.5	1.085	0.0026662	2.682	7.7	20.65
101.5	1.142	0.0009117	0.916	10.8	9.90	417.7	1.079	0.0035457	3.567	6.0	21.40

COUNTER FLOW											
Qc (act)	rho_c (rot)	mdot_c	C_c	DELTA.Tc	q_c	Qh (act)	rho_h (rot)	mdot_h	C_h	DELTA.Th	q_h
(scfh)	(kg/m3)	(kg/s)	(W/K)	(K)	(W)	(scfh)	(kg/m3)	(kg/s)	(W/K)	(K)	(W)
99.9	1.180	0.0009268	0.931	12.2	11.36	102.8	1.115	0.0009009	0.906	16.4	14.86
99.9	1.180	0.0009268	0.931	13.4	12.48	207.5	1.093	0.0017841	1.795	10.1	18.13
99.9	1.180	0.000927	0.932	13.4	12.48	312.6	1.084	0.0026654	2.681	7.5	20.11
99.8	1.181	0.0009271	0.932	13.1	12.21	417.9	1.078	0.0035441	3.565	5.7	20.32

Table B.1 - Processed Experimental Data

AIR PROPERTY DATA BASED ON AVERAGES OF:													
PARALLEL FLOW													
Cold T_film	Cold T_bulk	Cold c_p	Cold mu	Cold k_f	Cold nu	Cold Pr	Hot T_film	Hot T_bulk	Hot c_p	Hot mu	Hot k_f	Hot nu	Hot Pr
(°C)	(°C)	(J/kg-K)	(Ns/m2)	(W/m-K)	(m2/s)	--	(°C)	(°C)	(J/kg-K)	(Ns/m2)	(W/m-K)	(m2/s)	--
29.90125	25.1	1005	0.00001849	0.02587	0.00001607	0.7269	54.825	60.0	1006	0.00002008	0.0277	0.00001844	0.7211

COUNTER FLOW													
Cold T_film	Cold T_bulk	Cold c_p	Cold mu	Cold k_f	Cold nu	Cold Pr	Hot T_film	Hot T_bulk	Hot c_p	Hot mu	Hot k_f	Hot nu	Hot Pr
(°C)	(°C)	(J/kg-K)	(Ns/m2)	(W/m-K)	(m2/s)	--	(°C)	(°C)	(J/kg-K)	(Ns/m2)	(W/m-K)	(m2/s)	--
32.5375	39.1	1005	0.00001914	0.02607	0.00001631	0.7263	55.0375	60.0	1006	0.00002008	0.02772	0.00001986	0.721

Table B.2 - Air Property Data

Appendix C
Performance Data

Table C.1 Spreadsheet Calculations for Performance Data (#7 and #8 in Lab Manual)

PERFORMANCE DATA																				
PARALLEL FLOW																				
Qc (act) (scfh)	Qh (act) (scfh)	Tc,1 (in) (K)	Th,1 (in) (K)	Tc,2 (in) (K)	Th,2 (out) (K)	q_c (W)	q_h (W)	q_max (W)	Epsilon_c -	Epsilon_h -	delta_T_lm (K)	U_c W/m2-K	U_h W/m2-K	NTU_c -	NTU_h -					
100.9	102.7	298.3	333.2	305.5	316.3	6.63	15.33	31.64	0.209	0.484	20.54	7.19	16.61	0.356	0.823					
101.3	207.3	298.1	333.2	307.9	322.4	9.00	19.40	32.23	0.279	0.602	23.30	8.60	18.54	0.421	0.907					
101.5	312.5	298.3	333.2	308.9	325.5	9.72	20.65	32.00	0.304	0.645	24.63	8.79	18.67	0.430	0.915					
101.5	417.7	298.5	333.2	309.3	327.2	9.90	21.40	31.79	0.311	0.673	25.33	8.68	18.78	0.426	0.920					
COUNTER FLOW																				
Qc (act) (scfh)	Qh (act) (scfh)	Tc,1 (out) (K)	Th,1 (in) (K)	Tc,2 (in) (K)	Th,2 (out) (K)	q_c (W)	q_h (W)	q_max (W)	Epsilon_c -	Epsilon_h -	delta_T_lm (K)	U_c W/m2-K	U_h W/m2-K	NTU_c -	NTU_h -					
99.9	102.8	311.5	333.2	299.3	316.8	11.36	14.86	30.72	0.370	0.484	19.52	12.96	16.95	0.642	0.840					
99.9	207.5	312.7	333.2	299.3	323.1	12.48	18.13	31.58	0.395	0.574	22.11	12.57	18.26	0.606	0.880					
99.9	312.6	312.6	333.2	299.2	325.7	12.48	20.11	31.68	0.394	0.635	23.43	11.87	19.12	0.572	0.921					
99.8	417.9	312.2	333.2	299.1	327.5	12.21	20.32	31.77	0.384	0.640	24.51	11.09	18.46	0.534	0.890					
PERFORMANCE DATA																				
PARALLEL FLOW																				
Qc	Qh	Tc,1	Tc,2	Th,1	Th,2	Tm,c	Tm,h	rho,m,c	rho,m,h	Vbar,c	Vbar,h	Re,D,c	Re,D,h	Nu,c	Nu,h	h,c	h,h	U	NTU	epsilon
(scfh)	(scfh)	(°C)	(°C)	(°C)	(°C)	(°C)	(°C)	kg/m3	kg/m3	m/s	m/s					W/m2-K	W/m2-K	W/m2-K		
100.9	102.7	25.1	32.3	60.0	43.1	28.705	51.55	1.170	1.087	1.619	16.05	178.44	7048.99	6.67	24.98	10.11	85.33	9.59	0.439	
101.0	207.3	24.9	34.7	60.0	49.2	29.8	54.6	1.165	1.077	1.619	1741.61	13963.95	6.67	43.17	10.11	147.43	10.11	0.457		
101.5	312.5	25.1	35.7	60.0	52.3	30.4	56.15	1.163	1.072	1.619	48.14	1738.79	20845.92	6.67	59.48	10.11	203.14	10.32	0.468	
101.5	417.7	25.3	36.1	60.0	54.0	30.7	57	1.162	1.069	1.620	64.19	1737.57	27722.25	6.67	74.71	10.11	255.18	10.44	0.473	
COUNTER FLOW																				
Qc	Qh	Tc,1	Tc,2	Th,1	Th,2	Tm,c	Tm,h	rho,m,c	rho,m,h	Vbar,c	Vbar,h	Re,D,c	Re,D,h	Nu_c	Nu_h	h_c	h_h	U	NTU	epsilon
(scfh)	(scfh)	(°C)	(°C)	(°C)	(°C)	(kg/m3)	(kg/m3)	m/s	m/s							W/m2-K	W/m2-K	W/m2-K		
99.9	102.8	38.3	26.1	60.0	43.6	32.2	51.8	1.156	1.086	1.655	16.05	1706.47	7043.42	7.25	24.97	11.07	85.33	6.92	0.317	
99.9	207.5	39.5	26.1	60.0	49.9	32.8	59.95	1.154	1.076	1.658	31.10	1706.47	13948.81	7.25	43.13	11.07	147.40	7.33	0.327	
99.9	312.6	39.4	26.0	60.0	52.5	32.7	59.25	1.154	1.072	1.658	48.14	1706.76	20839.52	7.25	59.46	11.07	203.23	7.50	0.334	
99.8	417.9	39.0	25.9	60.0	54.3	32.45	57.15	1.155	1.069	1.657	64.19	1707.04	27709.55	7.25	74.68	11.07	255.26	7.59	0.339	

Appendix D

Hand Calculations

ME343 LAB10

DOTAMETER CORRECTION & HEAT XFER CALCULATIONS

$$\rho_{\text{ROT}} = \frac{P_{\text{ROT}}}{R T_{\text{ROT}}} \quad (\text{IDEAL AIR})$$

$P_{\text{ROT}} \approx P_{\text{ATM}}$, $T_{\text{ROT}} \approx \text{TEST SECTION EXIT TEMP}$

FOR COLD AIR @ $Q_h = 100 \text{ SCFM}$, PARALLEL FLOW:

$$\rho_{\text{ROT}} = \frac{101325 \text{ Pa}}{(287 \frac{\text{J}}{\text{kg} \cdot \text{K}})(305.45 \text{ K})} = 1.156 \frac{\text{kg}}{\text{m}^3}$$

$$\dot{t}_{\text{ROT}} = \sqrt{\frac{P_{\text{atm}}}{\rho_{\text{ROT}}}} \sqrt{\frac{T_{\text{ROT}}}{T_{\text{Cin}}}}$$

$\frac{P_{\text{atm}}}{\rho_{\text{ROT}}} \approx 1$; $\dot{t}_{\text{ROT}} = Q \text{ MEASURED}$; $T_{\text{atm}} \approx 300 \text{ K}$

FOR COLD AIR @ $Q_h = 100 \text{ SCFM}$, PARALLEL FLOW:

$$(Q_h)_{\text{ROT}} = (100 \text{ SCFM}) \sqrt{(1) \left(\frac{305.45 \text{ K}}{300 \text{ K}} \right)} = 100.9 \text{ SCFM}$$

$$\dot{m} = \rho_{\text{ROT}} \dot{V}_{\text{ROT}} = \rho_{\text{ROT}} (Q)_{\text{ROT}}$$

FOR COLD AIR @ $Q_h = 100 \text{ SCFM}$, PARALLEL FLOW:

$$\dot{m}_c = (1.156 \frac{\text{kg}}{\text{m}^3})(100.9 \frac{\text{ft}^3}{\text{hr}}) \left(\frac{0.7648 \text{ ft}}{\text{ft}} \right)^3 \left(\frac{\text{hr}}{3600 \text{ s}} \right) = 0.000917 \frac{\text{kg}}{\text{s}}$$

$$C = \dot{m} c_p$$

FOR COLD AIR @ $Q_h = 100 \text{ SCFM}$, PARALLEL FLOW:

$$C = (0.000917 \frac{\text{kg}}{\text{s}})(1005 \frac{\text{J}}{\text{kg} \cdot \text{K}}) = 0.922 \frac{\text{W}}{\text{K}}$$

$$q = \dot{m} c_p \Delta T = C \Delta T$$

FOR COLD AIR @ $Q_h = 100 \text{ SCFM}$, PARALLEL FLOW:

$$q_c = (0.922 \frac{\text{W}}{\text{K}})(32.3^\circ\text{C} - 25.1^\circ\text{C}) = 6.63 \text{ W}$$

→ NUMBER 7:

$$\epsilon_n = \frac{f_n}{f_{\max}}, \quad \epsilon_c = \frac{f_c}{f_{\max}}, \quad f_{\max} = C_{\min}(T_{h_i} - T_{c_i})$$

• FOR CASE OF LOWEST FLOW RATE, PARALLEL FLOW:
($Q_c, Q_h = 100$ (UNCORRECTED))

$$f_{\max} = 0.907 (60 - 25.1) = 31.6 \text{ W}$$

$$\epsilon_c = \frac{0.63}{31.6} = 0.209$$

$$\epsilon_n = \frac{15.33}{31.6} = 0.48$$

→ CONFIRMS EXPECTATION THAT $\epsilon_n > \epsilon_c$

• DETERMINE U :

$$f = UA\Delta T_{lm}, \quad \Delta T_{lm} = \frac{(\Delta T_2 - \Delta T_1)}{\ln\left(\frac{\Delta T_2}{\Delta T_1}\right)}$$

$$U = \frac{f}{A \Delta T_{lm}}$$

• FOR CASE OF $Q_c = Q_h = 100$ (UNCORRECTED) FOR PARALLEL PLATES:

$$U_c = \frac{f_c}{A \Delta T_{lm}} \quad A = \pi \left(\frac{D_0 + D_1}{2} \right) L \\ = \pi \left(\frac{0.953}{100} + \frac{0.811}{100} \right) (1.5) \left(\frac{1}{2} \right) \\ = 0.0415 \text{ m}^2$$

$$\rightarrow \Delta T_{lm} = \frac{(T_{h_2} - T_{c_2}) - (T_{h_1} - T_{c_1})}{\ln\left(\frac{T_{h_2} - T_{c_2}}{T_{h_1} - T_{c_1}}\right)} \\ = \frac{(316.3 - 305.5) - (333.2 - 298.3)}{\ln\left(\frac{316.3 - 305.5}{333.2 - 298.3}\right)} \\ = 20.54$$

$$U_c = \frac{0.63}{(0.0415)(20.54)} = 7.76 \frac{\text{W}}{\text{m}^2 \cdot \text{K}}$$

SIMILARLY:

$$U_n = \frac{q_n}{A \Delta T_{lm}} = \frac{15.33}{(0.0415)(20.54)}$$

$$U_n = 17.95 \text{ W/m}^2\text{-K}$$

NTU:

$$NTU = \frac{UA}{C_{min}}$$

- FOR CASE OF $Q_c = Q_h = 100$ (UNCORRECTED)
FOR PARALLEL PLATES:

$$NTU_c = \frac{U_c A}{C_{min}} = \frac{(7.76)(0.0415)}{0.907}$$

$$NTU_c = 0.355$$

→ SIMILARLY:

$$NTU_n = \frac{U_n A}{C_{min}} = \frac{(17.95)(0.0415)}{0.907}$$

$$NTU_n = 0.823$$

→ NUMBER \dot{m} :

$$\cdot \dot{T}_m = \frac{T_1 + T_2}{2} \implies \text{For } T_c (100, 100 \text{ sec}) - \text{PARALLEL}$$

$$T_c = \frac{25.1 + 32.3}{2} = 28.7^\circ\text{C}$$

$$\cdot \rho_m = \frac{P_{atm}}{R T_m} \implies \frac{101325 \text{ N/m}^2}{(287 \frac{\text{N}\cdot\text{m}}{\text{kg}\cdot\text{K}})(28.7 + 273.15 \text{ K})} = 1.169 \frac{\text{kg}}{\text{m}^3}$$

$$\cdot \bar{V} = \frac{\dot{m}}{\rho_m A_c} \implies \frac{0.000917}{(1.169) (\underbrace{\pi/4 (0.0266^2 - 0.00953^2)}_{\frac{\pi}{4} (D^2 - D_o^2)})}$$

$$\bar{V} = 1.619 \frac{\text{m}}{\text{s}}$$

$$\cdot R_{ed} = \frac{\rho \bar{V} D}{\mu} = \frac{(1.169)(1.619)(0.0266 - 0.00953)}{0.00001849}$$

$$R_{ed} = 1748$$

• Nu, c : → EVALUATED PLOT FOR REPORT #3
(PLOT OF TEMP VS AXIAL LOCATION)
FOUND THAT $T_w \approx \text{CONST}$. FOR CONST T_w , LAMINAR FLOW, $Nu_b = 6.67$

$$\cdot \bar{h}_c: \quad \overline{Nu}_{D_c} = \frac{\bar{h}_c D_h}{k} \implies \bar{h}_c = \frac{k}{D_h} \overline{Nu}_{D_c}$$

$$\bar{h}_c = \frac{0.02587}{0.01707} (6.67) \quad [=] \quad \frac{W}{\text{m}^2 \cdot \text{K}}$$

$$\bar{h} = 10.108 \frac{W}{\text{m}^2 \cdot \text{K}}$$

$$\cdot \frac{1}{UA_s} = \frac{1}{(hA)_n} + \cancel{R_w} + \frac{1}{(hA)_c}$$

$$U = \left[A_s \left(\frac{1}{(hA)_n} + \frac{1}{(hA)_c} \right) \right]^{-1}$$

$\hookrightarrow A_{s,n} = \pi D_i L \quad \hookrightarrow A_{s,c} = \pi D_o L$

$$= \left[\pi \left(\frac{0.00811 + 0.00953}{2} \right) (1.5) \left(\frac{1}{(35.3)(0.1038)} + \frac{1}{(16.1)(0.0441)} \right) \right]^{-1}$$

$$= 9.59 \frac{W}{\text{m}^2 \cdot \text{K}}$$

NTU:

$$\text{NTU} = \frac{UA}{C_{HIN}} = \frac{(9.59)(0.0415)}{0.907} = 0.439$$

LONG SURFACE AREA
 $A_s = \pi(D_o + D_i)L$

 ϵ :

$$\begin{aligned}\epsilon &= \frac{1 - \exp(-\text{NTU}(1 + C_r))}{1 + C_r} = 0.984 \\ &= \frac{1 - \exp(-0.439(1 + 0.984))}{1 + 0.984} \\ &= 0.293\end{aligned}$$